Ab Initio Study of the Isomeric Equilibrium of the HCN···H_2O and H_2O···HCN Hydrogen-Bonded Clusters

T. Malaspina,[†] E. E. Fileti,*[,‡] J. M. Riveros,[‡] and S. Canuto[†]

Instituto de Física, Universidade de São Paulo, CP 66318, 05315-970, São Paulo, SP, Brazil, and Instituto de Química, Universidade de São Paulo, Av Lineu Prestes 748, 05508-900, São Paulo, SP, Brazil

Received: May 6, 2006; In Final Form: June 30, 2006

An ab initio study of the stability, spectroscopic properties, and isomeric equilibrium of the hydrogen-bonded HCN···H_2O and H_2O···HCN isomers is presented. Density functional theory and perturbative second-order MP2 and coupled-cluster CCSD(T) calculations were carried out and binding energies obtained with correlation-consistent basis sets including extrapolation to the infinity basis set level. At the best theoretical level, CCSD-(T), the H_2O···HCN complex is more stable than the HCN···H_2O complex by ca. 6.3 kJ mol^{-1}. Rotational and vibrational spectra, including anharmonic corrections, are calculated. These calculated spectroscopic data are used to obtain thermochemical contributions to the thermodynamic functions and hence the Gibbs free energy. The relative free energies are used to estimate the equilibrium constant for isomerism. We find that under typical conditions of supersonic expansion experiments (T < 150 K) H_2O···HCN is essentially the only isomer present. Furthermore, our calculations indicate that the hydrogen-bonded cluster becomes favorable over the separated moieties at temperatures below 200 K.

Introduction

The structure and energetics of gas-phase clusters, including hydrogen-bonded complexes, is a recurrent topic of modern physical-chemistry.[1−4] Molecules having the nitrile group (R−C≡N) are of particular interest, because the lone pair on the nitrogen atom allows for hydrogen bond formation with a proton donor molecule.[4] The simplest nitrile system, namely HCN, can act as both a proton donor and proton acceptor system in cluster formation, as is the case for water and alcohol molecules. This makes possible, for instance, the formation of linear or cyclic chains of HCN.[4] Likewise, the interaction of HCN with water leads to at least two different structural motifs. In one, the HCN is the proton donor (H_2O···HCN), and in the other, HCN is the proton acceptor (HCN···H_2O). The former system was the first to be identified,[5,6] and it is now known to be the most stable.[7−10] The H_2O···HCN cluster has been experimentally characterized by microwave spectroscopy in two independent studies as reported by Fillery-Travis[5] and Gutowsky et al.[6] More recently,[8−10] both complexes have been investigated at the theoretical and experimental levels. For example, Heikkilä et al.[8] studied the infrared spectrum of these complexes in low-temperature argon matrixes by the FTIR technique and calculated the relative stability of the two isomers on the basis of ab initio calculations at the MP2/6-311++G(2d,2p) level. High-level calculations have also been used to determine the equilibrium structures, the energetics, and the cooperative effects on the properties of HCN−water clusters.[10,11] From these studies, the fact has emerged that the H_2O···HCN complex is indeed more stable than its isomer HCN···H_2O. Coupled-cluster calculations at the CCSD(T) level predict the relative stability to be ca. 5.0 kJ mol^{-1} [8] to ca. 7.4 kJ mol^{-1}.[10] This relative stability is very important in determining the precursor of long chains and also in the possible relative abundance of the two species. This is of further interest in the physical chemistry of planetary atmospheres[12] and in comets where the astrophysical properties may provide important clues regarding the formation of the Solar system.[13] Both water and hydrogen cyanide are common elements in planetary environments, and the relative abundance of the isomeric hydrogen-bonded water−cyanide clusters is of interest. In gas mixtures, the relative abundance of one isomer over the other is a sensitive function of the relative energies of the two isomers. Hence, a detailed consideration of the binding energies is crucial. It is thus desirable to have a systematic analysis of the relative binding energies of these two complexes. In the present work, this topic is addressed using current high-level ab initio methods in the limit of the infinite basis set. We present a systematic study of the stability of the H_2O···HCN and HCN···H_2O complexes calculating the binding energy of both systems using the aug-cc-pVXZ basis sets[14] with X = 2, 3, and 4 and extending the results to the infinite basis limit. The theoretical models considered in this manuscript include density functional theory (DFT),[15] perturbation-based Møller−Plesset, and coupled-cluster calculations.[16] In addition, rotation and vibration spectra are characterized including the anharmonic contribution. Anharmonic effects are known to be important in both water[17−22] and HCN[23−28] separately, and it is well-established that these effects are very important in describing the vibration frequencies of hydrogen-bonded systems.[20−22,29−36] Thus, we also present the expected infrared spectra, including anharmonic effects, for the H_2O···HCN and HCN···H_2O complexes and compare them directly with the experimental infrared spectra and obtain the spectral shift upon hydrogen bond formation. From these spectroscopic information, thermochemical data and gas-phase Gibbs free energy have been determined and compared for the two isomers.

* Corresponding author. E-mail: fileti@iq.usp.br. Fax: +55.11.3091-3888.
[†] Instituto de Física.
[‡] Instituto de Química.

10.1021/jp062780p CCC: $33.50
Published on Web 08/05/2006

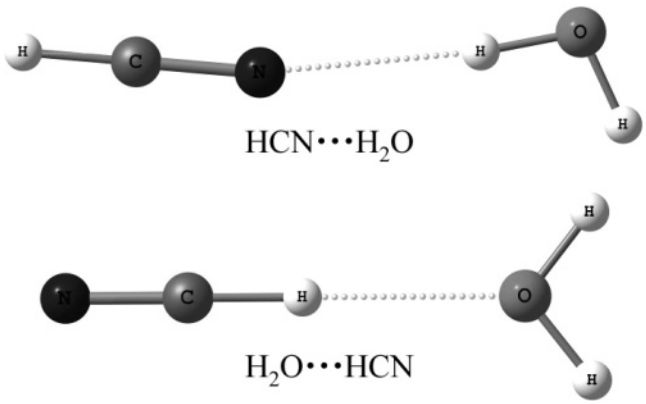

Figure 1. The structures of the HCN···H_2O and H_2O···HCN complexes.

Computational Details

The minimum-energy structures for the HCN···H_2O and H_2O···HCN complexes (and for the isolated species) were obtained using full geometry optimization with three different theoretical models: B3LYP/aug-cc-pVQZ, B3PW91/aug-cc-pVQZ, and MP2/aug-cc-pVTZ. The subsequent calculations of the vibrational frequencies testify that all structures reported are true minima. Single-point calculations for the optimized geometries were then performed using DFT, MP2, and coupled-cluster CCSD(T) theoretical models using the augmented correlation-consistent basis set aug-cc-pV*X*Z,[14] with $X = 2$, 3, and 4. The calculated binding energies were corrected for basis set superposition errors using the counterpoise correction,[37] and extrapolation schemes were employed to obtain these binding energies at the infinite basis set limit. Vibrational spectra for the complexes were initially calculated within the harmonic oscillator approximation, and corrections for anharmonicity were then determined using the method developed by Barone.[18,19] This method uses a second-order perturbation treatment based on quadratic, cubic, and semidiagonal quartic force constants.[18,19] All calculations were performed using the *Gaussian 03* suite of programs.[38]

Results

A. Structure. Figure 1 shows the general geometrical features calculated for the complexes. The HCN···H_2O complex has C_s symmetry, and the structure is in due agreement with previous determinations.[8,10] On the other hand, the H_2O···HCN complex has a very interesting structure that has attracted little attention.[5−8,10] Previous theoretical calculations found the water molecule to be out of the plane.[8,10] Experimentally, Gutowsky et al.[6] discussed this structure on the basis of their experimental results. They argued that the out-of-plane angle is about 20°, but the barrier is low enough that the zero-point vibrational motion extends over both minima. In fact, the experimental results suggest[6] that the complex is effectively planar. Although the nonplanar structure was found in earlier calculations,[8,10] all the theoretical models used here find the H_2O···HCN system to be planar and to have C_{2v} symmetry in agreement with experiment.[6] Table 1 shows the geometric parameters for these structures as determined by three different theoretical models, B3LYP/aug-cc-pVQZ, B3PW91/aug-cc-pVQZm and MP2/aug-cc-pVTZ. We can observe that the B3LYP/aug-cc-pVQZ and B3PW91/aug-cc-pVQZ models give very similar structures in both cases. As in other previous studies,[39,40] the C≡N distance obtained with MP2 is overestimated by ∼0.02 Å in both complexes with respect to the DFT values. The hydrogen bond distances, *R*(N···H) and *R*(H···O), are also in good agreement with the results obtained by Heikkilä et al.[8] at the MP2/6-311++G(2d,2p) level. The *R*(N···H) distance is 5% greater than *R*(H···O), and this is reflected in the binding energy as we will see in the next section. The observed trend is that a correlation exists between the hydrogen bond distance and the binding energy, i.e., the lower the distance, the larger the stability of the cluster. The O···C distance in the H_2O···HCN complex has been determined experimentally to be 3.128 Å,[6] while our calculated values range from 3.115 Å to 3.130 Å, in overall good agreement.

TABLE 1: Calculated Geometrical Parameters Obtained for HCN···H_2O and H_2O···HCN Complexes[a]

HCN···H_2O	B3LYP	B3PW91	MP2
R(H−C)	1.066	1.068	1.065
R(C≡N)	1.143	1.144	1.165
R(N···H)	2.125	2.140	2.090
R(H−O)	0.965	0.964	0.966
$R(\text{H}-\text{O})_{\text{free}}$	0.960	0.958	0.960
θ(C≡N···H)	171.3	171.0	171.4
α(C≡N···H−O)	2.8	3.4	2.4
H_2O···HCN	B3LYP	B3PW91	MP2
R(N≡C)	1.146	1.146	1.167
R(C−H)	1.074	1.076	1.072
R(H···O)	2.056	2.057	2.043
R(O−H)	0.961	0.959	0.962
θ(C−H···O)	180.0	180.0	180.0
α(H···OHH)	180.0	180.0	180.0

[a] DFT calculations used the aug-cc-pVQZ basis set, and the MP2 method used the aug-cc-pVTZ basis set.

TABLE 2: Binding Energy (kJ mol^{-1}) Obtained for the HCN···H_2O and H_2O···HCN Complexes[a]

HCN···H_2O	$X = 2$	$X = 3$	$X = 4$	extrapolated (see text)	relative energy
B3LYP	5.06	4.23	4.35	4.64[b]	
B3PW91	2.97	2.22	2.22	2.30[b]	
MP2	13.01	12.72	12.18	12.38[c]	
CCSD(T)	12.26	11.92	11.25	11.46[c]	
H_2O···HCN					
B3LYP	12.01	10.92	11.05	11.25[b]	6.61
B3PW91	9.96	9.08	9.04	9.08[b]	6.78
MP2	18.66	18.16	17.41	17.45[c]	5.06
CCSD(T)	18.66	18.20	17.45	17.45[c]	5.99

[a] Using different theoretical methods using the aug-cc-pvXZ basis set and the extrapolated energies including correction to the difference in zero-point vibrations. [b] Ref 41: $E_X = E_\infty + A_3X^{-3} + A_5X^{-5}$. [c] Ref 45: $E_\infty^{\text{cor}} = E_X^{\text{cor}}(1 - 2.4X^{-3})^{-1}$.

B. Relative Binding Energies. Table 2 shows the calculated results for the binding energies obtained by single-point calculations using four theoretical levels: B3LYP, B3PW91, MP2, and CCSD(T). For each level, we used three basis sets: aug-cc-pV*X*Z with $X = 2$ (D), 3 (T), and 4 (Q). The DFT calculations were performed using the optimized structures obtained with the aug-cc-pVQZ basis set, while MP2 and CCSD(T) single-point calculations were carried out with the MP2/aug-cc-pVTZ optimized structure. All values include the difference in zero-point vibrational energies and are also corrected for basis set superposition error.

The results obtained for the aug-cc-pV*X*Z basis set were extrapolated to the limit of infinite basis set. For the density functional results, the energy was directly extrapolated following the same scheme that was successfully used in previous calculations:[41] $E_X = E_\infty + A_3X^{-3} + A_5X^{-5}$. For the MP2 and

CCSD(T) methods, several approaches are available for extrapolating to the basis set limit.[42−45] In the present case, we have used the extrapolation scheme proposed by Varandas[45] that allows for the use of larger cardinal numbers: $E_{\infty}^{cor} = E_X^{cor}(1 - 2.4X^{-3})^{-1}$. The values obtained using these extrapolation schemes are reported in Table 2. The DFT results yield the lowest binding energies, similar to the results obtained in previous studies.[46] We also observe that for both complexes the binding energies obtained with B3PW91 are very small. This tendency of B3PW91 to give lower values for the binding energy as compared to the B3LYP was observed before in the analysis of the relative stability of the isomers of the AlP_3 molecule.[46] Despite the lower binding energy values for the separate isomers, we also see in Table 2 that the relative energies of the two isomers obtained using the two DFT methods are well-balanced. By comparison, the MP2 calculation yields the larger values for the binding energies but the smaller relative stability between the two isomers. In this respect, the MP2 results give a different numerical picture compared to the two DFT methods considered. CCSD(T) is the highest-order calculation and is expected to give the most balanced results. It predicts the $H_2O\cdots HCN$ complex to be more stable by 5.99 kJ mol^{-1}. For the particular case of the $H_2O\cdots HCN$ complex, the MP2 binding energies are close to the CCSD(T) values, indicating that higher-order electron correlation effects are small or cancel out such that their influence is of mild importance. This behavior has also been observed previously for other hydrogen-bonded complexes.[47] Including the extrapolated value, the MP2 method yields the larger binding energies, 12.38 and 17.45 kJ mol^{-1} for $HCN\cdots H_2O$ and $H_2O\cdots HCN$ complexes, respectively. Heykkilä et al.[8] have obtained these binding energies, not including ZPE, as 15.31 and 19.66 kJ mol^{-1} using the MP2/6-311++G(2d,2p) theoretical level. In all cases, the $H_2O\cdots HCN$ is more stable than the $HCN\cdots H_2O$ complex. This larger stability of the $H_2O\cdots HCN$ complex is in line with the two calculated hydrogen bond distances. The R(H···O) distance in the $H_2O\cdots HCN$ complex is around 0.05 Å smaller than the R(N···H) distance of 2.09 Å, indicating a stronger interaction. The energy difference between the two complexes using the basis set limit at the MP2 level is 5.06 kJ mol^{-1} and is 6.78 kJ mol^{-1} at the B3PW91 level. At the highest level, CCSD(T), with extrapolated results to the infinite basis limit, this difference is 5.99 kJ mol^{-1}. The average of all theoretical results using this infinite basis limit is 6.11 kJ mol^{-1}. This relative stability was obtained before by Heikkilä et al.[8] as 4.98 kJ mol^{-1}, whereas Rivelino et al.[10] obtained 7.49 kJ mol^{-1}. Our present result of 6.11 kJ mol^{-1} is between these two previous estimates.

C. Rotation and Vibration Analysis. After obtaining the equilibrium geometries, the moments of inertia are easily obtained and hence the rotational constants. These are shown in Table 3 and correlate well with the experimental results.[6] The harmonic vibrational spectrum for the $H_2O\cdots HCN$ and $HCN\cdots H_2O$ complexes have been studied previously using MP2 methods, and relatively good agreement with the experimental spectra was obtained for the frequency shifts upon hydrogen bond formation.[8,10] Here, we analyze the effects of the anharmonic contribution based on calculations beyond the harmonic approximation. These values are then used for obtaining the vibration contribution to the isomeric equilibrium. Presumably, more accurate values can be obtained for the calculated frequencies and the frequency shifts by inclusion of anharmonicity effects. Predictions regarding the intermolecular modes are expected to be less accurate because of the nature of the potential energy for these low-frequency vibrations. However, these very low energy modes are not expected to give any appreciable contribution to the vibration part of the enthalpy used in the determination of the isomeric equilibrium.

TABLE 3: Calculated Rotational Constants (in MHz) at Equilibrium (A_e, B_e, C_e) and in the Ground Vibrational State (A_0, B_0, C_0)

$HCN\cdots H_2O$	B3LYP	B3PW91	MP2	exptl[a]
A_e	425891.161	428538.329	430058.277	
B_e	3087.862	3081.866	3030.902	
C_e	3066.877	3060.881	3009.916	
A_0	390383.743	394892.621	353515.266	
B_0	3075.871	3093.858	3021.908	3045.589
C_0	3051.887	3078.868	3000.922	3020.258

$H_2O\cdots HCN$	B3LYP	B3PW91	MP2
A_e	526966.189	527026.147	481011.003
B_e	3261.742	3225.767	3249.750
C_e	3243.754	3204.781	3228.767
A_0	627834.359	624503.665	583647.949
B_0	3183.796	3120.839	3183.796
C_0	3159.812	3099.854	3159.812

[a] The experimental values are from ref 6.

The calculated spectrum for the isolated species including anharmonic contributions is shown in Table 4, along with the corresponding harmonic frequencies and the experimental values. The values in parentheses are the calculated intensities for the vibrational transitions. The anharmonic frequencies of HCN have recently been considered by Isaacson.[23] The low-frequency value of the bending mode δ_{HCN} was obtained experimentally[48] as 713 cm^{-1} and calculated here as 714 cm^{-1} using B3LYP and 722 cm^{-1} using B3PW91, while Isaacson[23] obtained 720 cm^{-1}; all of these values are in very good agreement. The MP2 results are less successful. In general, the DFT results agree well with each other and are in very good agreement with the experimental results. For H_2O, the numerical performance of the second-order MP2 is very good. Table 5 presents the calculated frequencies for the two hydrogen-bonded complexes. We observe that the very weak C≡N stretching mode (ν_{CN}) presents a sizable deviation that can presumably be attributed to the incorrect description of the triple bond character as discussed before. The anharmonic corrections are in the range of −204 cm^{-1} for the $\nu_{(OH)asymm}$ stretching mode (MP2, in $H_2O\cdots HCN$) to −164 cm^{-1} for the $\nu_{(OH)symm}$ stretching mode (B3PW91, in $H_2O\cdots HCN$) for the O—H (ν_{OH}). For the H—O—H bending (δ_{HOH}), the anharmonicity corrections are in the range of −58 (B3PW91, in $HCN\cdots H_2O$) to −43 cm^{-1} (B3PW91, in $H_2O\cdots HCN$). For the C—H (ν_{CH}) and C≡N stretching modes, these corrections are smaller, around −35 and −20 cm^{-1}, respectively. The HCN bending mode ($\delta_{(HCN)}$) displays the smallest correction. These corrections are reflected in a reduction in the difference between the experimental and calculated values from 3.5% to 1.6% in the case of the $HCN\cdots H_2O$ complex and from 3.5% to 1.9% in the case of the $H_2O\cdots HCN$ complex, at the B3PW91 level.

The anharmonic frequency shifts are also in good agreement with experimental values as can be seen in Table 6. The estimated experimental red shift of the frequency of the $\nu_{(OH)symm}$ mode is −44 cm^{-1}, while our calculated anharmonic value is −41 cm^{-1} at the MP2 level. The red shift of the frequency of the $\nu_{(OH)symm}$ mode is also well-described, −130 versus −124 cm^{-1}. Overall, the MP2 method has a better performance than DFT methods to describe the frequency shifts. The bonding O—H in the hydrogen bond is less red-shifted than its corresponding C—H (−41 versus −124 cm^{-1}), indicating that the hydrogen bond in the $H_2O\cdots HCN$ complex is stronger than that in the

TABLE 4: Harmonic and Anharmonic Vibrational Frequencies (in cm^{-1}) Calculated for the Isolated Species in Three Theoretical Levels with aug-cc-pVTZ Basis Set[a]

	B3LYP		B3PW91		MP2			
H_2O modes	harm	anharm	harm	anharm	harm	anharm	ref 23	exptl[b]
δ_{HOH}	1618(71)	1567	1621(71)	1570	1622(76)	1573		1590
$\nu_{(OH)symm}$	3795(4)	3617	3827(4)	3654	3804(5)	3621		3638
$\nu_{(OH)asymm}$	3905(61)	3715	3940(60)	3754	3938(63)	3744		3733
HCN modes								
$\delta_{(HCN)i}$	729(38)	714	736(38)	722	704(36)	692	720	713
$\delta_{(HCN)o}$	729(38)	714	736(38)	722	704(36)	692	720	713
ν_{CN}	2186(2)	2161	2194(1)	2168	1990(2)	1957	2097	2098
ν_{CH}	3450(68)	3318	3458(65)	3323	3452(66)	3327	3319	3312

[a] The i and o indices for the $\delta_{(HCN)}$ mode indicate bending in the plane and out of the plane, respectively. In parentheses are given the intensity (in km mol^{-1}) of the mode. [b] Experimental results for H_2O and HCN are from refs 48 and 49, respectively.

TABLE 5: Harmonic and Anharmonic Vibrational Frequencies (in cm^{-1}) Calculated for the HCN···H_2O Complex in Three Theoretical Levels with aug-cc-pVTZ Basis Set[a]

	B3LYP		B3PW91		MP2		MP2[b]	
HCN···H_2O modes	harm	anharm	harm	anharm	harm	anharm	harm	exptl[b]
δ_{HOH}	1640(53)	1584	1643(53)	1585	1642(47)	1589	1618	1629
$\nu_{(OH)symm}$	3738(234)	3569	3765(219)	3598	3754(195)	3580	3659	3594
$\nu_{(OH)asymm}$	3880(122)	3695	3913(116)	3726	3911(143)	3721	3799	3713
$\delta_{(HCN)i}$	739(38)	749	746(38)	735	710(40)	716	694	728
$\delta_{(HCN)o}$	740(35)	738	746(36)	749	711(36)	716	694	727
ν_{CN}	2202(83)	2171	2209(5)	2177	2009(0)	1968	1952	2109
ν_{CH}	3452(234)	3308	3459(78)	3311	3457(90)	3322	3324	3298
H_2O···HCN modes								
δ_{HOH}	1620(63)	1574	1623(61)	1579	1626(61)	1575	1595	1599
$\nu_{(OH)symm}$	3798(14)	3619	3828(14)	3664	3803(14)	3616	3700	3635
$\nu_{(OH)asymm}$	3905(86)	3708	3937(85)	3752	3933(91)	3729	3813	3740
$\delta_{(HCN)i}$	835(33)	818	840(32)	839	818(34)	792	834	815
$\delta_{(HCN)o}$	856(42)	846	862(42)	868	847(44)	812	816	827
ν_{CN}	2174(39)	2148	2179(39)	2148	1989(9)	1955	1933	2090
ν_{CH}	3323(376)	3166	3324(368)	3133	3353(361)	3203	3220	3182

[a] The i and o indices for the $\delta_{(HCN)}$ mode indicate bending in the plane and out of the plane, respectively. In parentheses are given the intensities of the modes. [b] Ref 8.

TABLE 6: Harmonic and Anharmonic Vibration Frequency Shifts (cm^{-1}) Calculated from Tables 4 and 5[a]

	B3LYP		B3PW91		MP2			
HCN···H_2O modes	harm	anharm	harm	anharm	harm	anharm	exptl[b]	exptl[c]
δ_{HOH}	22	16	21	14	20	16	39	38
$\nu_{(OH)symm}$	−57	−48	−62	−55	−50	−41	−44	−44
$\nu_{(OH)asymm}$	−25	−20	−27	−28	−27	−23	−23	−23
$\delta_{(HCN)i}$	10	35	9	13	6	23	15	8
$\delta_{(HCN)o}$	11	24	10	27	7	23	14	7
ν_{CN}	15	10	15	10	18	11	11	16
ν_{CH}	2	−10	2	−12	5	−4	−14	−6
H_2O···HCN modes								
δ_{HOH}	1	7	1	9	4	3	9	8
$\nu_{(OH)symm}$	3	2	1	10	−1	−6	−3	−3
$\nu_{(OH)asymm}$	0	−6	−2	−3	−5	−15	7	4
$\delta_{(HCN)i}$	106	104	104	117	115	100	102	107
$\delta_{(HCN)o}$	127	132	126	145	143	120	114	94
ν_{CN}	−13	−13	−15	−20	−1	−2	−8	−3
ν_{CH}	−127	−152	−133	−190	−98	−124	−130	−122

[a] The i and o indices for the $\delta_{(HCN)}$ mode indicate bending in the plane and out of the plane, respectively. [b] Refs 48 and 49. [c] Ref 8.

HCN···H_2O complex. This is corroborated by the comparison of the intermolecular O···N and O···C frequencies in both complexes, which is higher for H_2O···HCN than HCN···H_2O, 148 versus 136 cm^{-1}.

D. Cluster Abundance and Relative Percentage of Isomers. Our results are now extended to address two questions that bear a direct relationship to atmospheric and interstellar chemistry as well as to spectroscopic measurements of HCN···H_2O clusters: (a) what is the expected isomeric composition of H_2O···HCN and HCN···H_2O as a function of temperature, and (b) what is the temperature range where cluster formation becomes favorable?

The isomeric composition can be obtained from the equilibrium constant K for isomerization

$$\Delta G^\circ(\text{isomer}) = -RT \ln K$$

where ΔG°(isomer) is the difference between the gas-phase standard Gibbs free energy of the two isomeric species H_2O···HCN and HCN···H_2O. This difference can be calculated from the individual Gibbs free energy for each isomer

$$G = H - TS$$

by explicitly considering the thermal corrections to the thermodynamic functions using the well-known statistical mechanical formulation for gas-phase molecules.[38,50]

The corrections for the two isomeric species are expected to be very similar, and thus lead to significant cancellation in the thermal correction for the difference in the Gibbs free energies of the two isomers. Table 7 displays the calculated values at 298.15 K for different levels of theory along with the relative binding energies. For all levels of theory considered in this paper, the isomer in which water acts as the proton acceptor is energetically the more stable species. As seen in Table 2,

TABLE 7: Relative Stability (kJ mol^{-1}) of $H_2O\cdots HCN$ Compared to $HCN\cdots H_2O$, Considering the Thermochemical Contribution[a]

	B3LYP	B3PW91	MP2	CCSD(T)
ΔE	−6.69	−6.82	−5.44	−6.28
ΔE^b	−6.61	−6.78	−5.06	−5.99
ΔG	−5.56	−7.53	−5.48	−6.28[c]

[a] DFT results obtained with the aug-cc-pVQZ basis set and MP2 and CCSD(T) results with the aug-cc-pVTZ. Values at 1 atm and 298.15 K. [b] Using the extrapolated results to the infinite basis set limit (see text). [c] Estimated from the thermochemical corrections obtained with MP2/aug-cc-pVTZ.

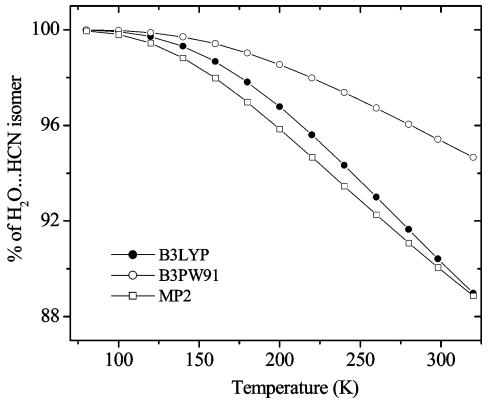

Figure 2. Temperature dependence of the relative percentage presence of $H_2O\cdots HCN$ in gas mixtures.

calculations at the MP2/aug-cc-pVTZ level indicate that the more stable isomer has a higher binding energy by 5.44 kJ mol^{-1}, whereas with the infinite-basis limit, at the MP2 level the difference in binding energies is calculated to be 5.06 kJ mol^{-1}. Inclusion of the thermochemical corrections for 298.15 K yields a relative Gibbs free energy of 5.48 kJ mol^{-1} at the MP2 level. The DFT results display a different behavior with thermochemical corrections to the B3LYP level calculations decreasing the difference in stability, whereas thermochemical corrections at the B3PW91 level increase the difference in stability at 298.15 K.

For the different levels of theory used in this study, we find that the calculated values for $\Delta G°$(isomer) at 298.15 K range from −5.44 to −7.53 kJ mol^{-1}. These values correspond to equilibrium constants of $9 \leq K \leq 21$ at 298.15 K, and the prediction that the $H_2O\cdots HCN$ form accounts for 90% to 95% of the clusters present in the equilibrium gas-phase mixtures at 298.15 K. Similar calculations for thermochemical corrections at lower temperatures lead to larger values of K_{isomer} and even higher relative abundance of the $H_2O\cdots HCN$ isomer as shown in Figure 2. Thus, we can predict that spectroscopic characterization of such clusters under supersonic expansion conditions ($T < 150$ K) would sample almost exclusively the $H_2O\cdots HCN$ isomer.

The second question to consider is the actual abundance of cluster formation from the individual monomeric H_2O and HCN species as a function of temperature.

$$H_2O(g) + HCN(g) \rightarrow H_2O\cdots HCN(g) \quad \Delta G°(H_2O\cdots HCN)$$

The $\Delta G°$(cluster) can be calculated at different temperatures from the binding energy of the $H_2O\cdots HCN(g)$ cluster at 0 K by calculating the appropriate thermochemical corrections for the reagents and the cluster. The calculated temperature variation of $\Delta G°(H_2O\cdots HCN)$ and $\ln K_{H_2O\cdots HCN}$ yield the data displayed in Figure 3. It is clear that $\Delta G°(H_2O\cdots HCN)$ is predicted to

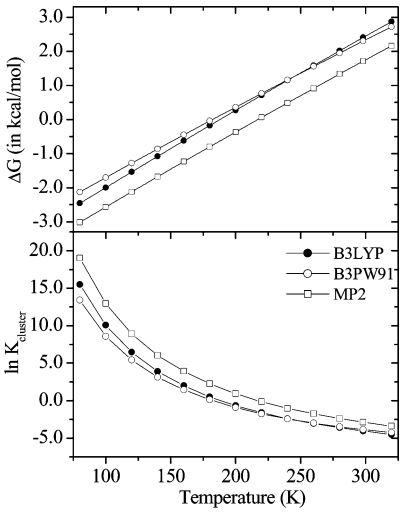

Figure 3. Temperature dependence of $\Delta G°(H_2O\cdots HCN)$ and $\ln K_{H_2O\cdots HCN}$.

become negative at temperatures below 200 K, thus leading to favorable cluster formation at these lower temperatures. This is particularly significant for interstellar conditions, given the fact that H_2O and HCN have been detected as important components of primitive atmospheres.[12,13]

Conclusions

The $HCN\cdots H_2O$ and $H_2O\cdots HCN$ complexes were studied using different theoretical models. Geometry optimizations were performed using B3LYP/aug-cc-pVQZ, B3PW91/aug-cc-pVQZ, and MP2/aug-cc-pVTZ. Binding energies for these complexes were obtained using aug-cc-pVXZ basis with $X = 2$, 3, and 4 with counterpoise corrections and taking into account zero-point energy (ZPE) differences. These results are extrapolated to the basis set limit. In addition, the high-level CCSD(T) method is used for the geometry optimized at the MP2/aug-cc-pVTZ level. The different theoretical results are in fair agreement with one another and show that the $H_2O\cdots HCN$ complex is more stable than the $HCN\cdots H_2O$ complex by ca. 6.0 kJ mol^{-1}. Rotational constants and vibrational spectra including harmonic and anharmonic contributions were also calculated for both isomeric complexes. Frequency shifts upon hydrogen bond formation have been obtained and compared with previous experimental and theoretical results. These calculated spectroscopic data have then been used to obtain thermochemical contributions for the Gibbs free energy. The relative free energies are used to estimate the equilibrium constant for isomerism. We find that under the conditions of supersonic expansion experiments ($T < 150$ K) $H_2O\cdots HCN$ is essentially the only isomer present. Our calculations also lead to the prediction that at temperatures below 200 K cluster formation through hydrogen bonding between H_2O and HCN becomes favorable over the separate moieties.

Acknowledgment. This work has been partially supported by CNPq and FAPESP (Brazil).

References and Notes

(1) Zwier, T. S. *Annu. Rev. Phys. Chem.* **1996**, *47*, 205.
(2) Bernstein, E. R., Ed. *Atomic and Molecular Clusters*; Elsevier: Amsterdam, 1990.
(3) Wilson, K. R.; Cavalleri, M.; Rude, B. S.; Schaller, R. D.; Catalon, T.; Nilsson, A.; Saykally, R. J.; Pettersson, L. G. M. *J. Phys. Chem. B* **2005**, *109*, 10194.
(4) Scheiner, S. *Hydrogen bonding: A theoretical perspective*; Oxford University Press: Oxford, 1997.

(5) Fillery-Travis, A. J.; Legon, A. C.; Willoughby, L. C. *Proc. R. Soc. London, Ser. A* **1984**, *396*, 405.
(6) Gutowsky, H. S.; Germann, T. C.; Augspurger, J. D.; Dykstra, C. E. *J. Chem. Phys*. **1992**, *96*, 5808.
(7) Turi, L.; Dannenberg, J. J. *J. Chem. Phys*. **1993**, *97*, 7899.
(8) Heikkilä, A.; Pettersson, M.; Lundell, J.; Khriachtchev, L.; Räsänen, M. *J. Phys. Chem. A* **1999**, *103*, 2945.
(9) Fileti, E. E.; Rivelino, R.; Canuto, S. *J. Phys. B: At. Mol. Opt. Phys.* **2003**, *36*, 399.
(10) Rivelino, R.; Canuto, S. *Chem. Phys. Lett*. **2000**, *322*, 207.
(11) Rivelino, R.; Canuto, S. *J. Phys. Chem. A* **2001**, *105*, 11260.
(12) Meot-Ner, M.; Speller, C. V. *J. Phys. Chem*. **1989**, *93*, 1697.
(13) Irvine, W. M.; Morvan, D. B.; Lis, D. C.; Matthews, H. E.; Biver, N.; Criviser, J.; Davies, J. K.; Dent, W. R. F.; Gautier, D.; Godfrey, P. D.; Keene, J.; Lovel, A. J.; Owen, T. C.; Phillips, T. G.; Rauer, H.; Schloerb, F. P.; Senay, M.; Young, K. *Nature (London)* **1996**, *383*, 418.
(14) Dunning, T. H., Jr. *J. Chem. Phys*. **1989**, *90*, 1007.
(15) Koch, W.; Holthausen, M. C. *A Chemist's Guide to Density Fuctional Theory*; Wiley-VCH: Weinheim, 2001.
(16) Jensen, F. *Introduction to Computational Chemistry*; Wiley: New York, 1999.
(17) Muñoz-Caro, C.; Niño, A. *J. Phys. Chem. A* **1997**, *101*, 4128.
(18) Barone, V. *J. Chem. Phys.* **2004**, *120*, 3059.
(19) Barone, V. *J. Chem. Phys*. **2005**, *122*, 014108.
(20) Chaban, G. M.; Jung, J. O.; Gerber, R. B. *J. Chem. Phys*. **1999**, *111*, 1823.
(21) Wright, N. J.; Gerber, R. B. *J. Chem. Phys*. **2000**, *112*, 2598.
(22) Wright, N. J.; Gerber, R. B.; Tozer, D. J. *Chem. Phys. Lett*. **2000**, *324*, 206.
(23) Isaacson, A. D. *J. Phys. Chem A* **2006**, *110*, 379.
(24) Isaacson, A. D. *J. Chem. Phys.* **2002**, *117*, 8778.
(25) Botschwina, P.; Schulz, B.; Horn, M.; Matuschewski, M. *Chem. Phys.* **1995**, *190*, 345.
(26) Allen, W. D.; Yamaguchi, Y.; Császár, A. G.; Clabo, D. A., Jr.; Remington, R. B.; Schaefer, H. F., III *Chem. Phys.* **1990**, *145*, 427.
(27) Almeida, W. B.; Hinchliffe, A. *THEOCHEM* **1990**, *204*, 153.
(28) Quapp, W. *J. Mol. Spectrosc.* **1987**, *125*, 122.
(29) Tokhadze, K. G.; Tkhorzhevskaya, N. A. *J. Mol. Struct*. **1992**, *270*, 351.
(30) Tokhadze, K. G.; Utkina, S. S. *Chem. Phys*. **2003**, *294*, 45.
(31) Biczysko, M.; Latajka, Z. *J. Phys. Chem. A* **2002**, *106*, 3197.
(32) Qian, W.; Krimm, S. *J. Phys. Chem.* **1996**, *100*, 14602.
(33) Antony, J.; von Helden, G.; Meijer, G.; Schimidt, B. *J. Chem. Phys.* **2005**, *123*, 014305.
(34) Chaban, G. M.; Gerber, R. B. *J. Chem. Phys.* **2001**, *115*, 1340.
(35) Brauer, B.; Gerber, R. B.; Kabeláč, M.; Hobza, P.; Bakker, J. M.; Riziq, A. G.; Vries, M. S. *J. Phys. Chem. A* **2005**, *109*, 6974.
(36) Chaban, G. M.; Gerber, R. B. *J. Phys. Chem. A* **2000**, *104*, 2772.
(37) Boys, S. F.; Bernardi, F. *Mol. Phys.* **1970**, *19*, 553.
(38) Frisch, M. J.; Trucks, G. W.; Schlegel, H. B.; Scuseria, G. E.; Robb, M. A.; Cheeseman, J. R.; Montgomery, J. A., Jr.; Vreven, T.; Kudin, K. N.; Burant, J. C.; Millam, J. M.; Iyengar, S. S.; Tomasi, J.; Barone, V.; Mennucci, B.; Cossi, M.; Scalmani, G.; Rega, N.; Petersson, G. A.; Nakatsuji, H.; Hada, M.; Ehara, M.; Toyota, K.; Fukuda, R.; Hasegawa, J.; Ishida, M.; Nakajima, T.; Honda, Y.; Kitao, O.; Nakai, H.; Klene, M.; Li, X.; Knox, J. E.; Hratchian, H. P.; Cross, J. B.; Bakken, V.; Adamo, C.; Jaramillo, J.; Gomperts, R.; Stratmann, R. E.; Yazyev, O.; Austin, A. J.; Cammi, R.; Pomelli, C.; Ochterski, J. W.; Ayala, P. Y.; Morokuma, K.; Voth, G. A.; Salvador, P.; Dannenberg, J. J.; Zakrzewski, V. G.; Dapprich, S.; Daniels, A. D.; Strain, M. C.; Farkas, O.; Malick, D. K.; Rabuck, A. D.; Raghavachari, K.; Foresman, J. B.; Ortiz, J. V.; Cui, Q.; Baboul, A. G.; Clifford, S.; Cioslowski, J.; Stefanov, B. B.; Liu, G.; Liashenko, A.; Piskorz, P.; Komaromi, I.; Martin, R. L.; Fox, D. J.; Keith, T.; Al-Laham, M. A.; Peng, C. Y.; Nanayakkara, A.; Challacombe, M.; Gill, P. M. W.; Johnson, B.; Chen, W.; Wong, M. W.; Gonzalez, C.; Pople, J. A. *Gaussian 03*, revision D.01; Gaussian, Inc.: Wallingford, CT, 2004.
(39) Kryachko, E. S.; Nguyen, M. T. *J. Phys. Chem A* **2002**, *106*, 4267.
(40) Fileti, E. E.; Rissi, E. A.; Canuto, S. *Theor. Chem. Acc*. **2003**, *110*, 360.
(41) Costa Cabral, B. J.; Canuto, S. *Chem. Phys. Lett*. **2005**, *406*, 300.
(42) Thrular, D. G. *Chem. Phys. Lett.* **1998**, *294*, 45.
(43) Laschuk, E. F.; Livotto, P. R. *J. Chem. Phys.* **2004**, *121*, 12146.
(44) Lee, J. S. *Theor. Chim. Acta* **2005**, *113*, 87.
(45) Varandas, A. J. C. *J. Chem. Phys*. **2000**, *113*, 8880.
(46) Malaspina, T.; Coutinho, K.; Canuto, S. *Chem. Phys. Lett*. **2005**, *411*, 14.
(47) Fileti, E. E.; Chaudhuri, P.; Canuto, S. *Chem. Phys. Lett*. **2004**, *400*, 494.
(48) Bentwood, R. M.; Barnes, A.; Orville-Thomas, W. *J. Mol. Spectrosc.* **1980**, *84*, 391.
(49) Smith, A. M.; Coy, S. L.; Klemperer, W.; Lehmann, K. K. *J. Mol. Spectrosc.* **1989**, *134*, 134.
(50) McQuarrie, D. A. *Statistical Thermodynamics*; Harper and Row: New York, 1973.